

Figure S1

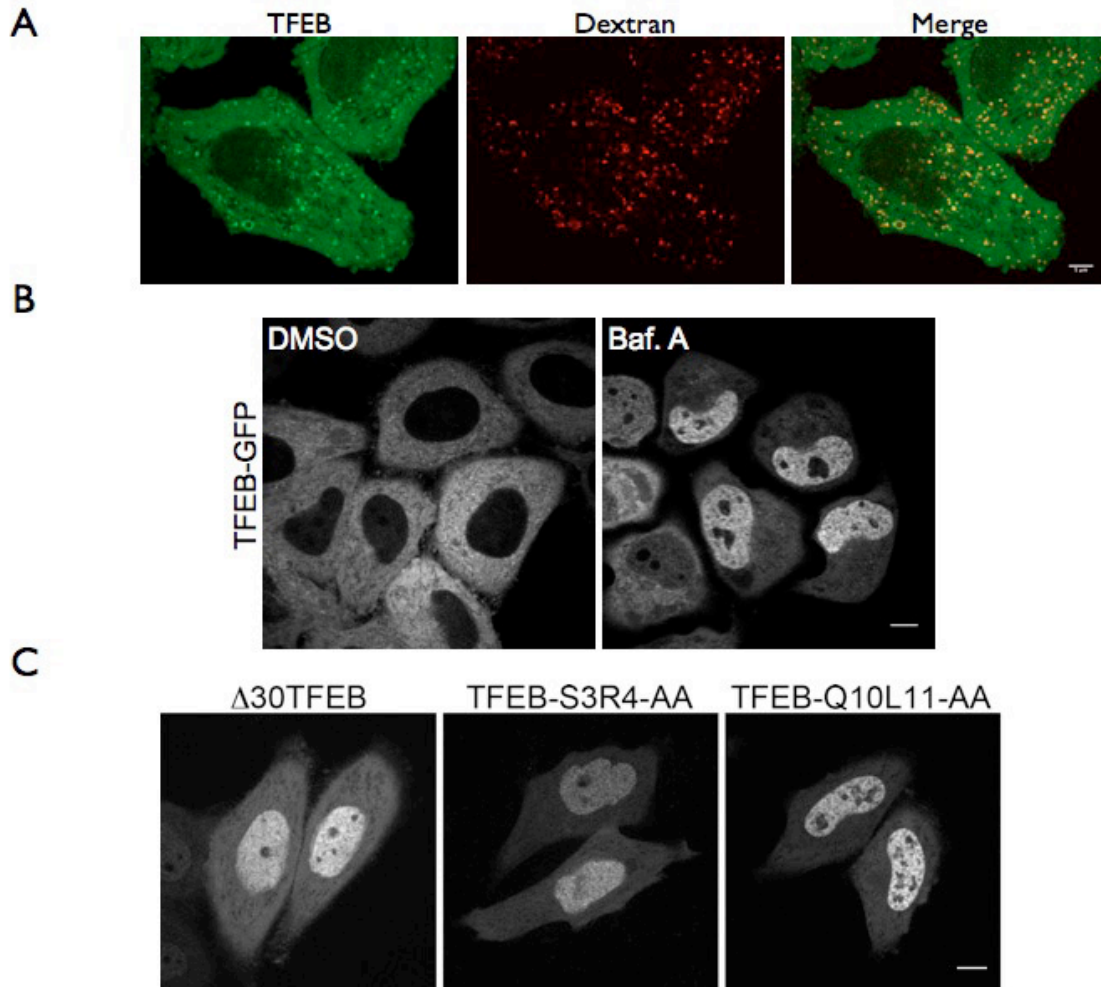


Fig. S1. Regulation of TFEB localization by lysosomal status. **(A)** Spinning disk confocal images showing the co-localization between TFEB-GFP and lysosomes labeled by Alexa 594-dextran. N=2 experiments, images are representative of the majority of cells observed. Scale bar = 5 μ m. **(B)** Spinning disk confocal images of HeLa M cells stably expressing TFEB-GFP following incubation (15 hours) with vehicle control (0.1% DMSO, left) or bafilomycin A (100 nM, right). N=3, images are representative of the majority of cells observed. **(C)** Spinning disk confocal imaging of HeLa M cells

transiently transfected with the indicated TFEB-GFP mutants. N =3 experiments, images are representative of the majority of cells observed. Scale bars= 10 μ m for B and C.

Figure S2

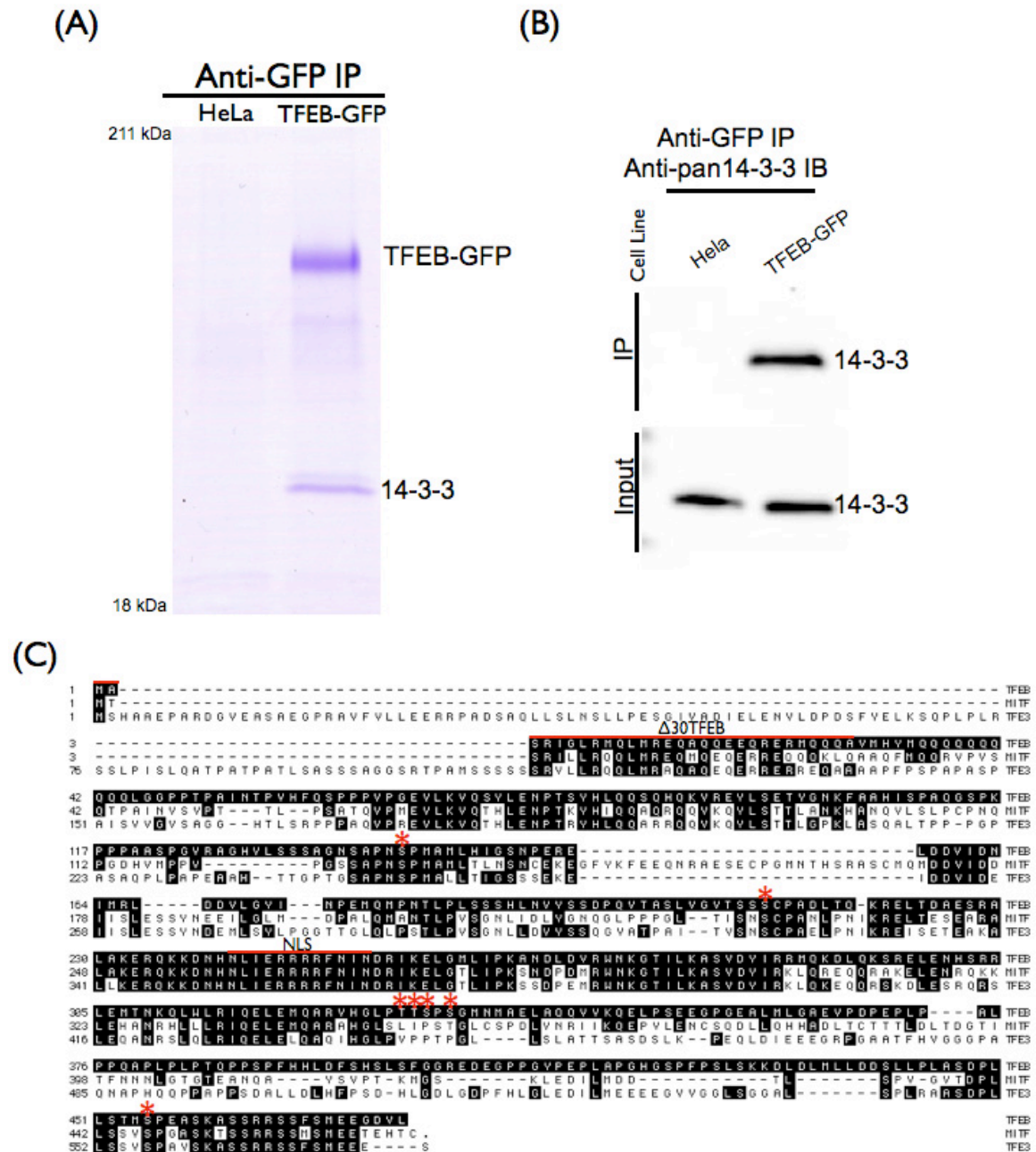


Fig. S2. 14-3-3 proteins are major binding partners of TFEB. (A) Coomassie stained SDS-PAGE gel showing the results of anti-GFP immunoprecipitations from control HeLa M cells or a TFEB-GFP expressing stable HeLa M cell line (n=3). (B) Immunoblot of anti-GFP immunoprecipitates using a pan-14-3-3 antibody shows the selective

enrichment of 14-3-3 isoforms in the material isolated from the TFEB-GFP stable cell line. The total fraction lanes were loaded with the equivalent of 1% of the material that was used for the corresponding immunoprecipitations (n=3). (C) Alignment of human TFEB, MITF (isoform D) and TFE3 sequences. Shading indicates sequences matching TFEB. The regions comprising the Δ 30 mutant of TFEB and the NLS are highlighted by red lines and the locations of Ser¹⁴², Ser²¹¹, Thr³³⁰, Thr³³¹, Ser³³², Ser³³⁴ and Ser⁴⁵⁵ in TFEB are highlighted by red asterisks.

Figure S3

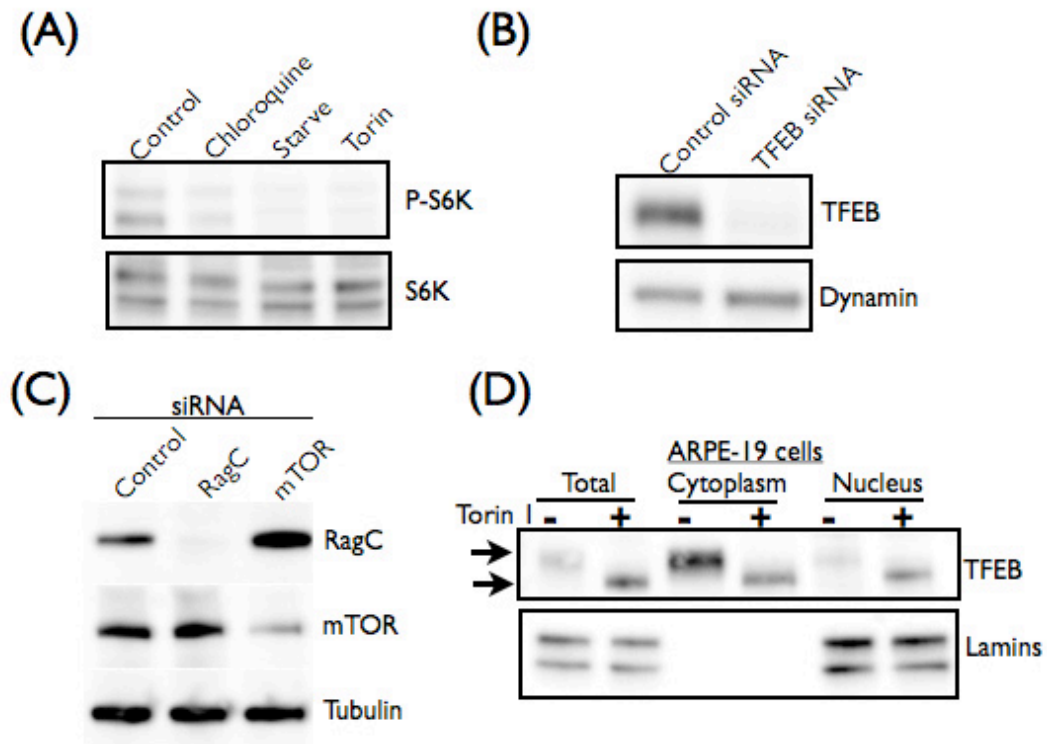


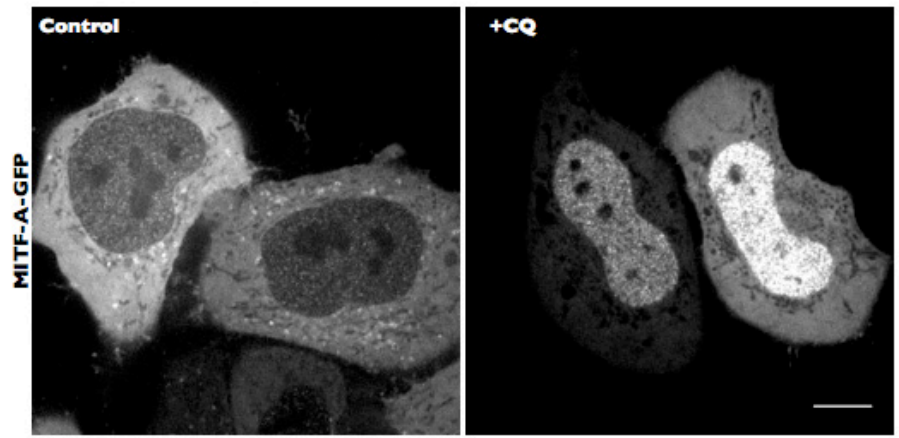
Fig. S3. Relationship between TFEB, mTOR and lysosomes. **(A)** Phospho-S6 kinase (P-S6K, Thr³⁸⁹) and total S6K immunoblots on lysates from cells receiving the indicated treatments (as described for Fig. 3D, n=2). **(B)** Immunoblot from HeLa cells transfected with control or TFEB siRNA demonstrates the specificity of the TFEB antibody purchased from Bethyl Laboratories (n=3). The blot was re-probed for dynamin to demonstrate equal sample loading. **(C)** Immunoblots showing efficiency of RagC and mTOR knockdowns (n=3). **(D)** Immunoblotting of subcellular fractions of ARPE-19 cells treated \pm torin 1 (2 μ M, 2 hours). Arrows highlight the migration difference that arises due to torin 1 treatment (n=3).

Figure S4

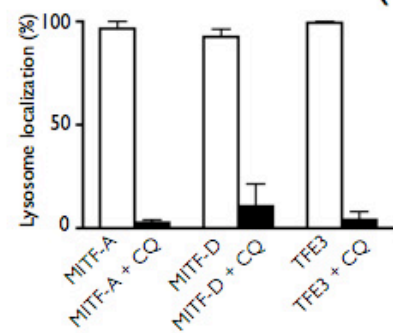
(A)



(B)



(C)



(D)

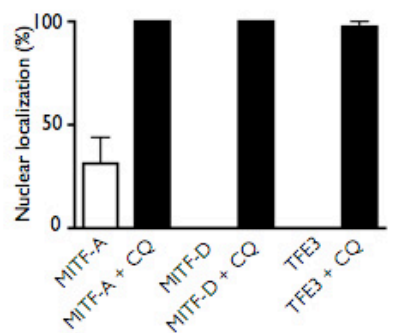


Fig. S4. MITF and TFE3 localization is sensitive to lysosome status. (A) Alignment of TFEB with MITF-A, D and M isoforms. Shading indicates sequences matching TFEB.

The regions comprising the $\Delta 30$ mutant of TFEB and the NLS are highlighted by red lines and the locations of Ser¹⁴², Ser²¹¹, Thr³³⁰, Thr³³¹, Ser³³², Ser³³⁴ and Ser⁴⁵⁵ in TFEB are highlighted by red asterisks. **(B)** Spinning disk confocal imaging of HeLa M cells expressing MITF-A-GFP \pm CQ treatment (50 μ M, 15 hours). Scale bar = 10 μ m. **(C)** Percentage of cells exhibiting lysosomal localization. n=3 experiments, 30-40 cells/condition/experiment. **(D)** Percentage of cells showing nuclear enrichment. n=3 experiments, 30-40 cells/condition/experiment.

Movie S1. Imaging of TFEB-GFP under basal conditions. Images from transfected HeLa M cells were acquired by spinning disk confocal imaging at 0.25 Hz and played back at 15 frames/second. Scale bar = 10 μm .